ADVANCED FUNCTIONAL MATERIALS
www.afm-journal.de

A Tumor Targeted Chimeric Peptide for Synergistic Endosomal Escape and Therapy by Dual-Stage Light Manipulation

*Kai Han, Qi Lei, Hui-Zhen Jia, Shi-Bo Wang, Wei-Na Yin, Wei-Hai Chen, Si-Xue Cheng, and Xian-Zheng Zhang**

In this study, a pH sensitive chimeric peptide is developed to codeliver a photosensitizer, protoporphyrin IX (PpIX), and plasmid DNA simultaneously. In the presence of matrix metalloproteinase-2 (MMP-2), the chimeric peptide undergoes the process of hydrolysis of PLGVR peptide sequence, exfoliation of PEG, and increase of positive charges. As a result, the chimeric peptide can be preferentially uptaken by MMP-2 rich tumor cells. To realize synergistic effect of drug and gene delivery, a dual-stage light irradiation strategy is developed, i.e., the short time light irradiation can efficiently enhance the endosomal escape of the chimeric peptide/PpIX/DNA complexes by the formation the reactive oxygen species (ROS), resulting in synergistic endosomal escape and improved DNA expression. In addition, due to the screened phototoxicity of PpIX, short time light irradiation does not lead to detectable changes in the cell viability. After the gene transfection, the screened phototoxicity of PpIX is subsequently stimulated by long time irradiation to achieve high synergistic efficacy of photodynamic and gene therapies. Both in vitro and in vivo studies confirm the chimeric peptide-based nanocarrier with a good synergistic effect is a promising nanoplatform for tumor treatments.

1. Introduction

Synergistic therapy holds considerable appeal in transporting various bioactive substances to target sites with elicited biological functions, enhanced therapeutic efficacy and minimal side effects.[1–4] Despite great effort has been devoted to develop ideal nanoplatforms that can incorporate various bioactive substances, the further development of synergistic therapy is still hampered by the intracellular obstacles such as cell membranes and endo/lysosomes.[5] To address the issue of endo/lysosomal barrier, "proton sponge" effect has been proposed to circumvent the endosomal trap.[6] However, some pioneering studies have corroborated that the "proton sponge" effect alone is not suffcient for endosomal disruption.[7] On the other hand, satisfactory therapeutic index of various bioactive substances cannot be realized with ease, particularly for antitumor drugs and genetic materials.[8,9] Since the high toxicity of traditional antitumor drug could always decrease the biological activity of cells, leading to partial sacrifice of the expression efficacy of genetic materials. Construction of the ingenious nanoplatforms that can achieve a satisfactory synergistic effect between antitumor drugs and genetic materials is still highly desirable and critical challenging.

Recently, photodynamic therapy has rapidly attracted much attention, mostly because of the precisely controllable phototoxicity via regulating the light irradiation condition, such as the irradiation time and intensity.[10] And light as a safe, noninvasive, and high spatiotemporal resolved energy source can reach to almost all parts of the body through external sources or catheterization.[11] Besides, when the photosensitizer (PS) was under light irradiation, the formation of ROS can disrupt of the endo/lysosomal membranes by photochemical internalization (PCI), thereby leading to improved cytoplasmic delivery of bioactive substances.[12–14] Unfortunately, limited work were done in the field of PCI related gene delivery to date.[15,16] And PS acted only as the endosomal destroyer, the inherent quality as a tumor executioner under long time light irradiation was always ignored in the majority of previous studies.

In addition, nanocarriers, especially cationic nanocarriers, should possess a tumor-triggered cleavable shielding surface since the cationic carriers always failed to discern healthy cells from diseased ones due to the electrostatic interaction, leading to unwanted side effects and reduced therapeutic index.[17–19]

Keeping all these issues in mind, in this study, we fabricated a pH sensitive chimeric peptide Fmoc-12-aminododecanoic acid-H_8R_8-PLGVR-PEG_8 (Fmoc-ADDA-H_8R_8-PLGVR-PEG_8, chimeric peptide in brief) to encapsulate the photosensitizer PpIX and DNA simultaneously. As illustrated in **Scheme 1**, at the physiological pH, this amphipathic chimeric peptide contained

K. Han, Q. Lei, H. Z. Jia, S. B. Wang, W. N. Yin, W. H. Chen, Prof. Dr. S. X. Cheng, Prof. X. Z. Zhang
Key Laboratory of Biomedical Polymers of Ministry of Education & Department of Chemistry
Wuhan University
Wuhan 430072, China
E-mail: xz-zhang@whu.edu.cn
Prof. X. Z. Zhang
Collaborative Innovation Center of Chemical Science and Engineering (Tianjin)
Tianjin 300072, China

DOI: 10.1002/adfm.201403190

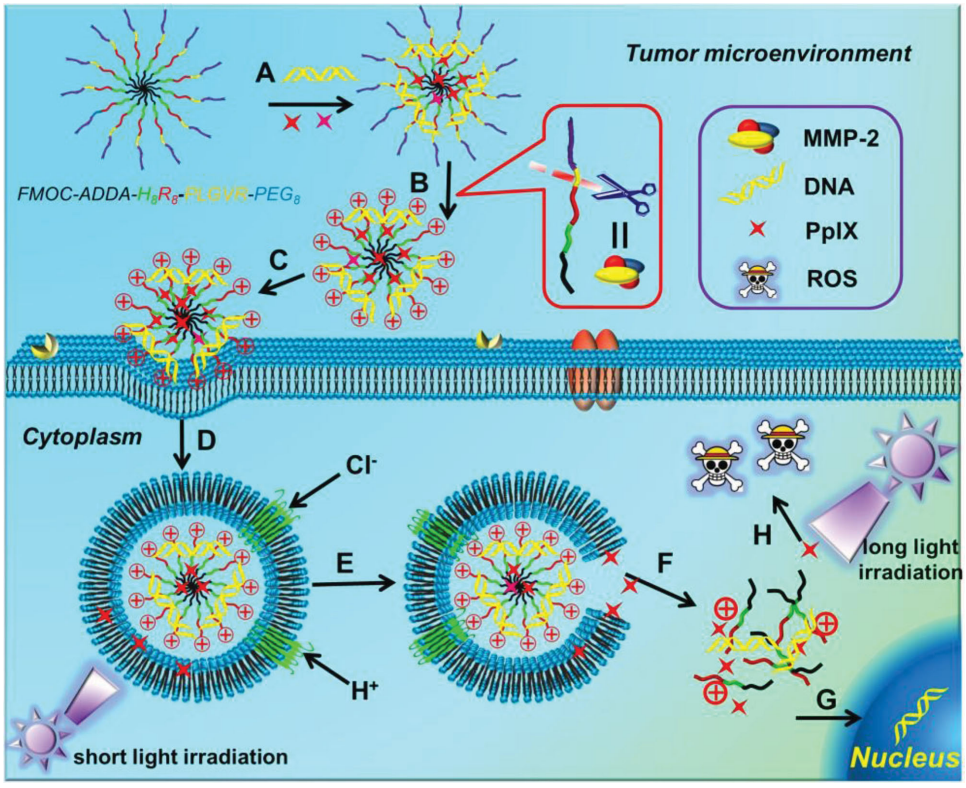

Scheme 1. Schematic diagram of the chimeric peptide/PpIX/p53 system. A) Encapsulation of PpIX and DNA; B) PEG detachment under MMP-2 enzyme; C) endocytosis of complexes mediated by electrostatic interaction; D) formation and acidification of endosomes; E) endosomal escape via "proton sponge" effect and PCI effect under short time light irradiation; F) diffusion through the cytoplasm; G) nuclear translocation and gene expression; H) phototoxicity of PpIX under long time light irradiation.

the Fmoc-ADDA-H_8 sequence as a hydrophobic motif to load PpIX and the CPP (cell penetrating peptide) sequence R_8 to bind the DNA. Besides, PEG was decorated to the outer shell of chimeric peptide via the MMP-2 substrate peptide (PLGVR) linker, which could be cleaved at tumor site and make the cationic CPP sequence exposed, leading to the specific uptake by tumor cells. After entering the endo/lysosomes, the protonation of H_8 sequence initiated endosomal escape to some extent. Meanwhile, the release of PpIX accelerated. Importantly, for the first time, we proposed a dual-stage light irradiation strategy to realize synergistic endosomal disruption (via "proton sponge" and PCI effect) and photodynamic/therapeutic gene-based tumor cell ablation. We demonstrated the high therapeutic index of the cooperative nanoplatform both in vitro and in vivo in a murine model.

2. Results and Discussion

2.1. Preparation and Characterization of Chimeric Peptide and PpIX or/and DNA Loaded Chimeric Peptide

The chimeric peptide was synthesized using standard fluorenylmethyloxycarbonyl solid phase peptide synthesis method. The product was characterized by electrospray ionization–mass spectrometry (ESI–MS). The theoretical molecular weight was 3728.1 (Figure S1, Supporting Information), and the multiple charge peaks were found at 1865.9 $[M+2H]^{2+}$, 1244.2 $[M+3H]^{3+}$, respectively.

As an ideal nanoplatform to codeliver the PpIX and gene, the nanocarrier should possess the capacity to encapsulate PpIX as well as DNA. In this study, PpIX was encapsulated in chimeric peptide via a solvent evaporation method. The UV–vis spectrum revealed that the PpIX loaded chimeric peptide exhibited strong absorption even above 630 nm (Figure S2, Supporting Information), which makes photodynamic therapy in deep tissue possible. In addition, due to the hydrophobic interaction between PpIX and chimeric peptide hydrophobic core, PpIX could be effectively encapsulated in the chimeric peptide. The drug loading efficiency (DLE) and entrapment efficiency (EE) values at pH 7.4 were 50% and 8.9%, respectively. Moreover, relatively slow drug release rate was observed at the physiological pH (pH 7.4). On the contrary, the drug release rate was accelerated significantly when the pH was decreased to 5.0 (**Figure 1**A), which corresponded to the pH of acidic subcellular organelles of endo/lysosomes. This discrepancy was attributed to the rapid protonation of H_8 sequence at the weak acidic environment, thereby leading to the enhanced hydrophilicity of chimeric peptide and loosened of the hydrophobic core.

The capacity of chimeric peptide and PpIX loaded chimeric peptide for plasmid DNA condensation was studied by agarose gel electrophoresis assay using pGL-3 DNA as a reporter gene

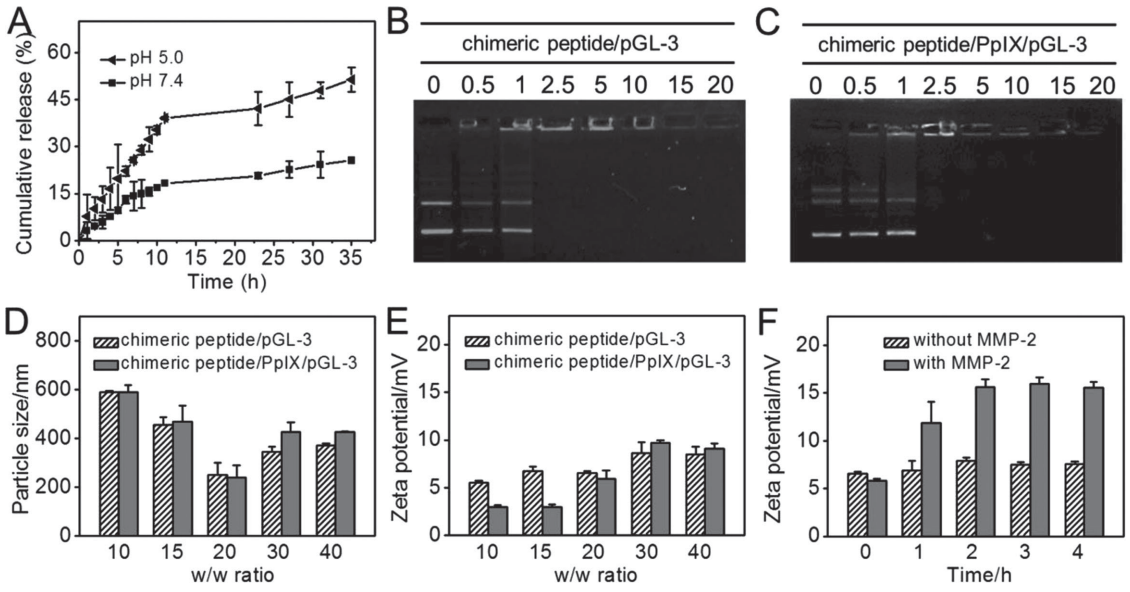

Figure 1. A) In vitro drug release behavior of PpIX loaded chimeric peptide at different pHs (pH 7.4 and 5.0). B,C) The agarose gel electrophoresis assay, D) particle size (pH 7.4) and E) zeta potential (pH 7.4) of chimeric peptide/pGL-3 complexes and chimeric peptide/PpIX/pGL-3 complexes at various w/w ratios. (E) Zeta potentials of chimeric peptide/pGL-3 complexes at w/w ratio of 20 in the absence of MMP-2 enzyme and after coincubation with MMP-2 enzyme for different time. Data are presented as mean ± S.D. ($n = 4$).

(pGL-3 in brief). As shown in Figure 1B, the mobility of pGL-3 was completely retarded by the chimeric peptide at a rather low w/w ratio of 2.5, suggesting the satisfactory DNA binding ability of chimeric peptide via electrostatic interaction. And the encapsulation of PpIX did not change the capacity of chimeric peptide for condensing DNA (Figure 1C). Furthermore, hydrodynamic particle size and zeta potential of the complexes at various w/w ratios were also determined (Figure 1D,E). Negligible difference was observed among the chimeric peptide/pGL-3 complexes and chimeric peptide/PpIX/pGL-3 complexes in both hydrodynamic particle size and zeta potential. It was also found that with the increasing of w/w ratio, the hydrodynamic particle size decreased dramatically and then reached a platform, and the zeta potential increased slowly. It was probably due to the fact that although more compact complexes could form when the content of chimeric peptide increased, the surface potential of complexes was still effectively shielded by PEG shell.[20] And this speculation was further verified by the measurement of zeta potential of chimeric peptide/pGL-3 complexes in the presence of the MMP-2 enzyme (Figure 1F). After addition of MMP-2, the zeta potential increased remarkably as expected which increased from 6 to 15 mV in 1 h. Apparently, the PLGVR sequence was hydrolyzed in the presence of MMP-2 enzyme, leading to the exfoliation of the PEG shell. As a result, the exposure of the cationic R_8 sequence caused the increased zeta potential.[21]

In light of the fact that the morphology of nanoparticle could influence the cellular uptake,[22] the morphology of the chimeric peptide encapsulated with PpIX or/and pGL-3 in the absence of MMP-2 enzyme and after coincubation with MMP-2 enzyme was observed by transmission electron microscopy (TEM). As shown in Figure S3 and S4 (Supporting Information), the morphological changes of various samples were negligible after incubation with MMP-2 enzyme. The well dispersed nanoparticles showed a spherical shape with a particle size of around 30 nm. The loading of drug did not change the size dramatically, while the DNA binding decreased the size owing to the formation of compact complexes. Similar results were found in dynamic light scattering (DLS) (Table S1, Supporting Information). It should be pointed out that the particle size observed by TEM was smaller than that measured by DLS. This difference was ascribed to the fact that TEM samples were observed in vacuum state, leading to the shrinkage of samples.[4,23]

2.2. MMP-2 Responsive Luciferase Expression and Cellular Uptake

Encouraged by the characteristics of the chimeric peptide in encapsulating PpIX and plasmid DNA, we further investigated the luciferase expression of pGL-3 mediated by chimeric peptide in squamous cell carcinoma (SCC-7) and African green monkey SV40-transfected kidney fibroblast cell (COS7) in the presence of 10% fetal bovine serum (FBS). **Figure 2**A revealed that the chimeric peptide could induce satisfactory luciferase expression at a w/w ratio of 20 in SCC-7 cells, which was comparable to the gold standard 25 kDa polyethylenimine (PEI). However, the luciferase expression was decreased to some extent in COS7 cells (Figure 2B). This result was attributed to the different uptake content of the chimeric peptide/pGL-3 complexes in the two cell lines. It was known that MMP-2 enzyme was secreted abundantly in the SCC-7 tumor cells, so the PLGVR sequence could be hydrolyzed in SCC-7 cells.[22] Subsequently, the PEG shell detached, leading to the increase of the positive charge on the surface of complexes, which was in favor of the cellular uptake of complexes owing to the negative charge of cell membrane.[17]

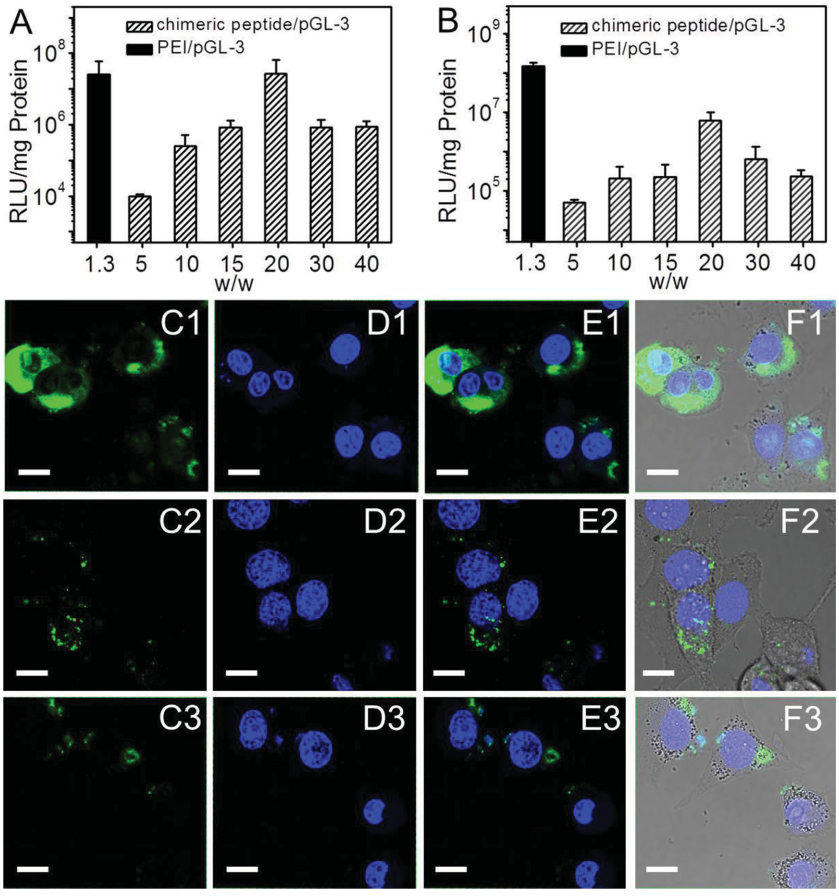

Figure 2. Luciferase expression mediated by chimeric peptide/pGL-3 complexes in A) SCC-7 cells and B) COS7 cells. 25 kDa PEI was used as control. Data are presented as mean ± S.D. ($n = 4$). Cellular uptake of chimeric peptide/pGL-3 complexes (w/w ratio 20) in (C1–F1) SCC-7 cells in the absence of MMP-2 inhibitor, (C2-F2) SCC-7 cells in the presence of MMP-2 inhibitor and (C3–F3) COS7 cells were determined by CLSM. Green channel: YOYO-1 labeled chimeric peptide/pGL-3 complexes. Blue channel: Hoechst 33342 labeled nucleus. E1, E2, and E3: the emerged images of green and blue signals. The scale bar was 10 μm.

This conjecture was further proved via confocal laser scanning microscopy (CLSM) and flow cytometry. From CLSM observation, the complexes were prepared by YOYO-1 labeled pGL-3. As compared with COS7 cells (Figure 2C3), an evidently stronger and larger area of green fluorescence was observed in SCC-7 cells (Figure 2C1). Clearly, the cellular uptake content of complexes in SCC-7 cells was significantly higher than that in COS7 cells. Moreover, once the MMP-2 inhibitor (1,10-phenanthroline monohydrate) was added, the intensity and area of green fluorescence in SCC-7 decreased (Figure 2C2). This finding substantially demonstrated that the relative higher cellular uptake content in SCC-7 cells was due to the MMP-2 responsiveness of the chimeric peptide. Furthermore, the quantitative determination of the cellular uptake of complexes via flow cytometry (**Figure 3**) revealed that the percentage of positive SCC-7 cells in the absence of MMP-2 inhibitor was over fivefold higher than that of positive COS7 cells. And the percentage of positive SCC-7 cells in the presence of MMP-2 inhibitor was significantly decreased, which was similar to that of positive COS7 cells. All these results were in consistence with the luciferase expression.

2.3. Photochemical Internalization Induced Endosomal Escape and Gene Transfection

After cellular internalization, the complexes were expected to enter organelle endo/lysosomes. The acidic environment and the existence of various enzymes in endo/lysosomes are hostile to bioactive substances. Rapid endosomal escape ability plays a crucial role in therapeutic effect. Herein, the endosomal escape behavior of the complexes was investigated by CLSM. The pGL-3 was labeled with YOYO-1, and the endo/lysosomes were stained with LysoTracker Blue. Fmoc-ADDA-R_8-PLGVR-PEG_8 without H_8 sequence was used as a negative control (ESI–MS in Figure S5, Supporting Information). After 6 h incubation with SCC-7 cells, the control peptide/pGL-3 complexes were mostly entrapped in the endo/lysosomes (**Figure 4**B3), which was evidenced by the highly overlapping of blue (endo/lysosomes) and green (peptide/pGL-3 complexes) fluorescences. In contrast, although some blue and green fluorescences were also overlapped, certain chimeric peptide/pGL-3 complexes had already escaped from endo/lysosomes since the isolated distribution of blue and green fluorescences could be observed (Figure 4C3). The endosomal escape of chimeric peptide/pGL-3 complexes was due to the "proton sponge" effect mediated by the chimeric peptide. The protonation of H_8 sequence in chimeric peptide/pGL-3 complexes prevented acidification process of endosomes to some extent. And then more protons and counter ions were transported into endosomes via ATP enzyme to further acidify the vesicles. As a result, the dramatically increased osmotic pressure triggered the enlargement of endosomes as well as the enhanced membrane permeability, leading to certain endosomal escape of complexes.[24]

To test our hypothesis that PpIX could further enhance the efficacy of endosomal escape via PCI effect, the distribution of chimeric peptide/PpIX/pGL-3 complexes in SCC-7 cells under light irradiation for various time intervals was also observed via CLSM. As shown in Figure 4D4, the endosomal escape behavior of chimeric peptide/PpIX/pGL-3 complexes was similar to that of chimeric peptide/pGL-3 complexes when the light irradiation was 0 min, i.e., only certain blue and green fluorescences were separate. However, after light irradiation (8 min or 15 min), the green fluorescence was distributed evenly in the cytoplasm (Figure 4E3,F3), suggesting the majority of chimeric peptide/PpIX/pGL-3 complexes escaped into the cytoplasm after short time light irradiation. This diffusive pattern of distribution is consistent with the previous reports.[6,25] It should be

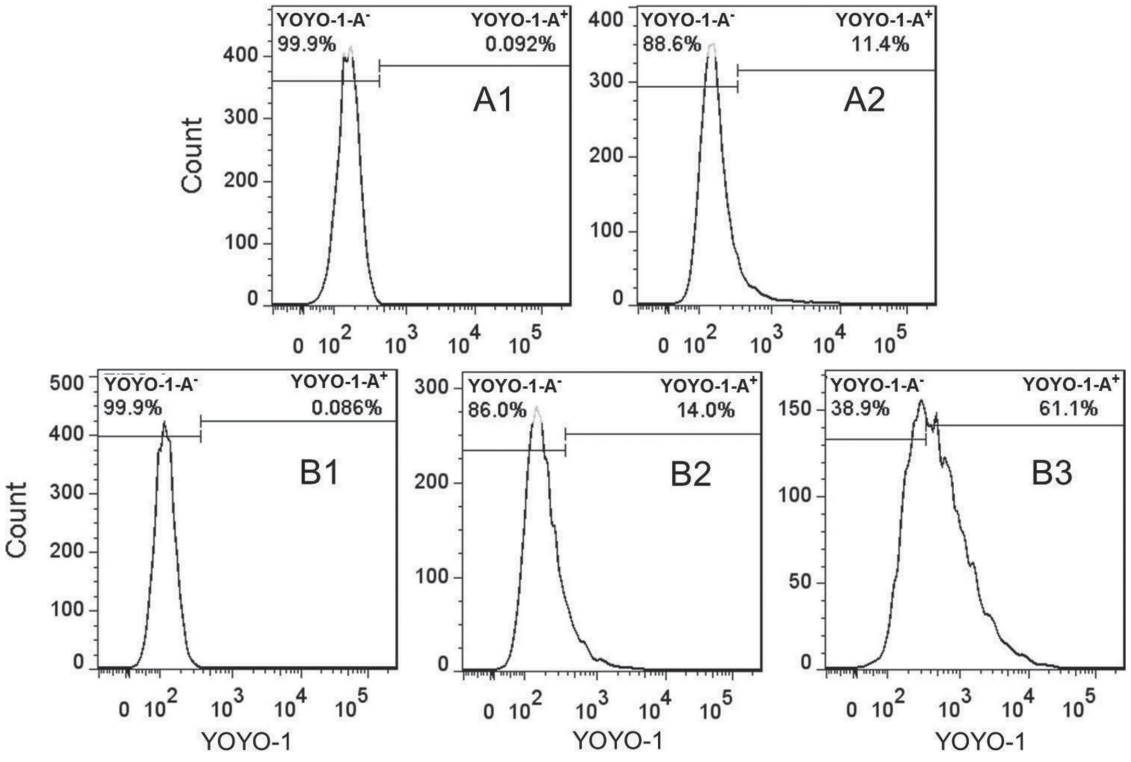

Figure 3. Cellular uptake behaviors of chimeric peptide/pGL-3 complexes in different cell-lines were determined by flow cytometer. A2) COS7 cells; B2) SCC-7 cells in the presence of MMP-2 inhibitor; B3) SCC-7 cells in the absence of MMP-2 inhibitor. (A1) and (B1) (chimeric peptide alone) were the negative controls, respectively. The w/w ratio was 20.

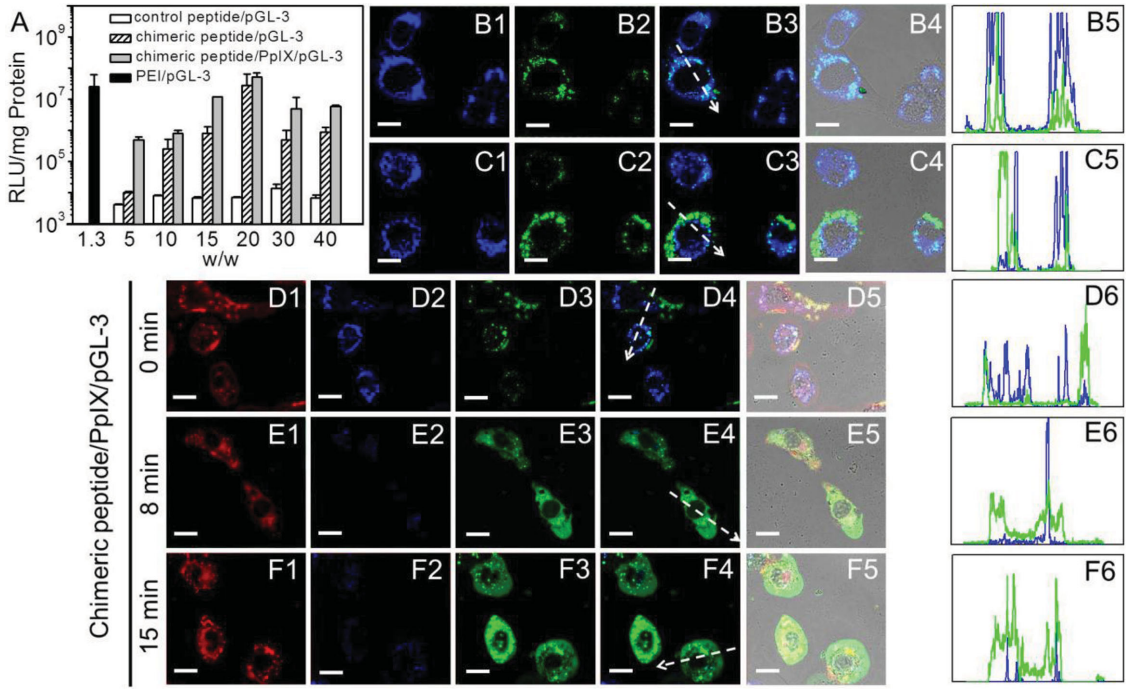

Figure 4. A) Luciferase expression mediated by various samples in SCC-7 cells. 25 kDa PEI was used as control. Data are presented as mean ± S.D. (n = 4). Endosome escape behaviors were observed by CLSM and the corresponding fluorescence-intensity-profile analysis. B1–B5) control peptide/pGL-3 complexes; C1–C5) chimeric peptide/pGL-3 complexes. D1–D6,E1–E6,F1–F6) chimeric peptide/PpIX/pGL-3 complexes with 0, 8, and 15 min light irradiation, respectively. (B4), (C4) and (D5–F5) were the emerged images. Blue channel: LysoTracker Blue; Green channel: YOYO-1 labeled chimeric peptide/pGL-3 complexes. Red channel: PpIX. The scale bare was 15 μm.

noted that the blue fluorescence of endo/lysosomes decreased dramatically (Figure 4E2,F2). As we know, the "proton sponge" effect could only enlarge the endosomal vesicles but not burst them.[7,26] However, the ROS could disrupt the membrane structure.[27] The accelerated release of PpIX in acidic endosomes under short time light irradiation induced the formation of ROS, leading to light-selective endosomal disruption and release of complexes into the cytoplasm. Furthermore, the colocalization efficacy between various samples and endosomes was further evaluated by fluorescence-intensity-profile analysis (Figure 4).[28] These results were consistent with their endosomal escape behaviors observed via CLSM.

The endosomal escape ability was also reflected by the luciferase expression of pGL-3. As shown in Figure 4A, owing to the "proton sponge" effect, the chimeric peptide mediated significantly higher gene transfection efficacy in SCC-7 cells compared with the control peptide, i.e., Fmoc-ADDA-R_8-PLGVR-PEG_8. Moreover, the gene transfection was further improved when the chimeric peptide/PpIX/pGL-3 complexes were light irradiated for 8 min after internalization for 6 h, which was even twofold higher than that mediated by 25 kDa PEI. Obviously, PCI-induced endosome escape under short time light irradiation could efficiently enhance the gene expression. On the other hand, it was worth noting that different from the traditional antitumor drugs that always showed high toxicity even at a low dose, PpIX with short time light irradiation had negligible influence in the cell viability (Figure S6, Supporting Information) and DNA bioactivity during DNA expression, which is the prerequisite for efficient gene transfection.

Additionally, it could also be observed that the red fluorescence and green fluorescence overlapped well (Figure 4D1–F1, D3–F3), implying the chimeric peptide could transport PpIX and DNA into the same cells efficiently. And this was further quantified by the flow cytometry (**Figure 5**). 40.3% cells were double-positive cells, which presented a majority of the cells. Taken together, the chimeric peptide based nanocarrier could codeliver the photosensitizer and the genetic materials to the target tumor cells, and then successfully escape from the endosomal trap under short time light irradiation to mediate gene transfection.

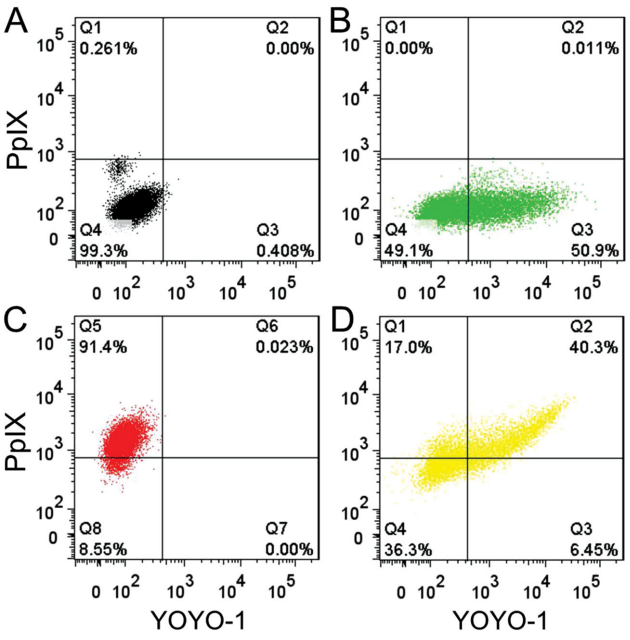

Figure 5. Codelivery of PpIX and gene by chimeric peptide was determined by two-color flow cytometry in SCC-7 cells. The w/w ratio of chimeric peptide/pGL-3 complexes was 20. A) Chimeric peptide as a negative control; B) YOYO-1 labeled chimeric peptide/pGL-3 complexes (green fluorescence positive); C) PpIX loaded chimeric peptide (red fluorescence positive); D) YOYO-1 labeled chimeric peptide/PpIX/pGL-3 complexes.

2.4. In Vitro Cytotoxicity Assessment

In order to get direct insight into synergetic efficacy between photodynamic and gene therapies, the cytotoxicity in vitro was determined using p53 DNA as a therapeutic gene. For comparison, we evaluated the cytotoxicity of chimeric peptide and PpIX and/or p53 loaded chimeric peptide. Unlike the 25 kDa PEI that presented serious cytotoxicity, the chimeric peptide did not exhibit apparent cytotoxicity and above 90% cells was still survived even when the concentration of peptide was 200 mg L^{-1} (**Figure 6**A).

Besides, p53 DNA alone has negligible cytotoxicity (data not shown), the chimeric peptide/p53 complexes resulted in cell growth inhibition due to the chimeric peptide mediated expression of p53 protein, which induced the apoptosis of tumor cells (Figure 6B). Once the PpIX was introduced, the cytotoxicity increased when the cells got 8 min light irradiation after 6 h internalization. Considering that chimeric peptide/PpIX/pGL-3 complexes had negligible cytotoxicity with 8 min light irradiation (Figure S6, Supporting Information), the enhanced cytotoxicity was mainly due to the PCI induced endosomal escape and improved gene transfection. Furthermore, it was also found that PpIX loaded chimeric peptide showed limited cytotoxicity without light irradiation (Figure 6C). After irradiation with visible light for 60 min, cytotoxicity was dramatically elevated, and the IC_{50} (the concentration that caused 50% inhibition of cellular growth) was 0.8 mg L^{-1}. The significant phototoxicity demonstrated the efficient generation of plenty of ROS by PpIX loaded chimeric peptide under long time irradiation.

The cytotoxicity of the chimeric peptide/PpIX/p53 complexes with dual-light irradiation was further investigated. As shown in Figure 6D, the chimeric peptide/PpIX/p53 complexes exhibited higher cytotoxicity than either PpIX loaded chimeric peptide or chimeric peptide/p53 complexes. And the synergistic efficacy was quantified by the combination index (CI_x), which were below 1 at 50%, 60%, and 70% of cell viabilities (Figure 6E), suggesting the synergy between PpIX and p53. The satisfactory synergy underlined the fact that the ROS generated by PpIX under short time light irradiation did not influence the biological activity of p53 DNA severely. In contrast, the PCI effect enhanced transfection of therapeutic gene. It was probably due to the compartmentalization of PpIX and p53 DNA, i.e., PpIX was encapsulated in the hydrophobic inner core while the p53 DNA was incorporated in the cationic shell. On the other hand, the phototoxicity of PpIX could be activated by long time light irradiation, which could further exhibit photodynamic therapeutic efficacy.

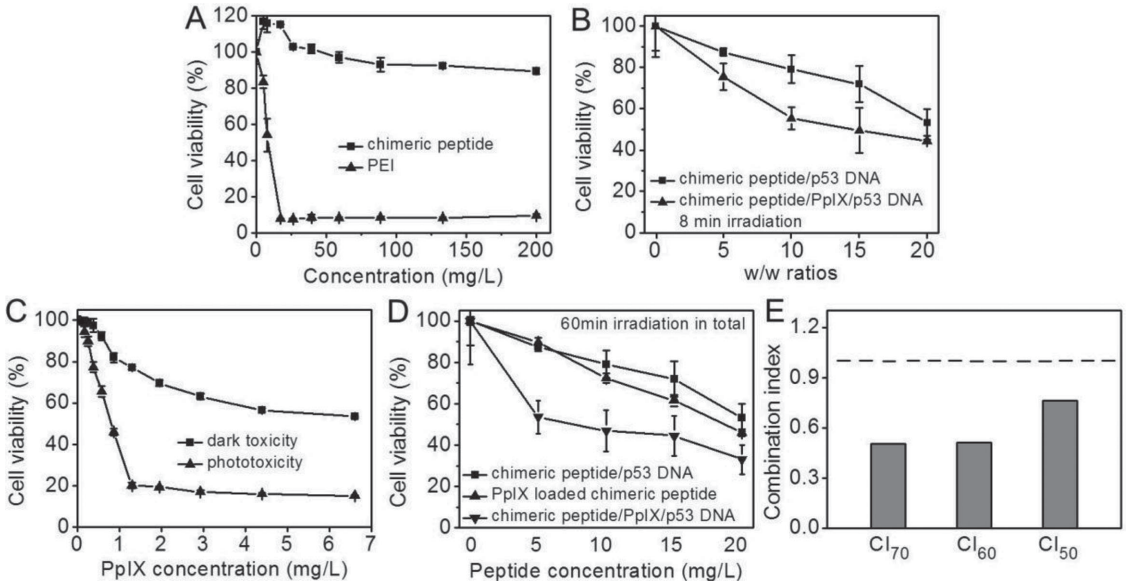

Figure 6. In vitro cell viability after different treatments: A) chimeric peptide and 25 kDa PEI; B) chimeric peptide/p53 complexes and chimeric peptide/PpIX/p53 complexes with 8 min light irradiation after 6 h internalization; C) PpIX loaded chimeric peptide without or with 60 min light irradiation; D) chimeric peptide/PpIX/p53 complexes with dual-stage light irradiation (8 + 52 min). Chimeric peptide/p53 complexes and PpIX loaded chimeric peptide with light irradiation (60 min) were used as controls. (The total light irradiation time was the same to different samples). Data are presented as mean ± S.D. (n = 6). E) The CI values at 50%, 60%, and 70% cell growth.

2.5. In Vivo Antitumor Efficacy

To demonstrate the feasibility of cooperative nanoplatform for tumor treatment in vivo, the long-term antitumor efficacy in treatment of a human xenograft tumor (SCC-7 cells) was investigated using nude mouse as an animal model. 630 nm He–Ne laser was used as the light source which was confirmed to be biosafety when the irradiation time was 30 min (Figure S7, Supporting Information). With dual-stage light irradiation, chimeric peptide/PpIX/p53 complexes showed the most significant tumor growth inhibition (**Figure 7**A). And the chimeric peptide encapsulated with individual therapeutic component presented remarkably less effective tumor growth inhibition. Similar results were also found in the tumor weights (Figure 7C) and intuitional tumor images (Figure 7D) at the 15th day. Meanwhile, after post-treatment of the chimeric peptide/PpIX/p53 complexes, there was no obvious change of the mouse body weight (Figure 7B), suggesting the negligible systemic toxicity of the complexes. Furthermore, standard hematoxylin and eosin (H&E) staining of the tumor tissues at the 15th day after treatment of various samples was also performed. As shown in **Figure 8**, only limited portion of tumor cells were apoptosis/necrosis after applying either PpIX loaded chimeric peptide or chimeric peptide/p53 complexes. On the contrary, in chimeric peptide/PpIX/p53 complexes-treated mice, the majority of cells in tumor tissue were killed. All these results supported a considerable evidence of the efficient in vivo antitumor activity of the chimeric peptide based nanoplatform.

3. Conclusion

In summary, we designed and fabricated a pH sensitive chimeric peptide with MMP-2 responsibility. This chimeric peptide could efficiently transport the photosensitizer (PpIX) and DNA to the targeted tumor cells. After cellular internalization, satisfactory endosomal escape was achieved due to the "sponge effect" of H_8 and "PCI effect" of PpIX under short time light irradiation, which ensured the high expression of therapeutic gene. And the long time irradiation after gene transfection activated the phototoxicity of PpIX, which killed the tumor cells further. The dual-stage light irradiation strategy demonstrated here addressed the bottlenecks of synergistic therapy, i.e., endosomal escape as well as the interference among antitumor drug toxicity, cell bioactivity, and gene transfection. This strategy should open a window in the design of cooperative nanoplatforms for the synergetic treatment of tumor.

4. Experimental Section

Materials: Detailed material information was provided in our previous article.[29] Additionally, Fmoc-PEG_8-OH was provided by Zhoubei Technology Co. Ltd. (Hangzhou, China). PpIX was purchased from Aladdin Reagent Co. Ltd. (China). Matrix metalloproteinases (MMP-2) was obtained from RD-SYSTEMS. LysoTracker Blue was provided by Xiamen Bioluminor Biotechnology Co. Ltd. (China). 1,10-phenanthroline monohydrate were provided by Aladdin Reagent Co. Ltd. (Shanghai, China).

Synthesis of Peptides: Both the peptides of Fmoc-ADDA-H_8R_8-PLGVR-PEG_8 and Fmoc-ADDA-R_8-PLGVR-PEG_8 were synthesized using standard fluorenylmethyloxycarbonyl solid phase peptide synthesis method. The peptide sequences were linked to a 2-chlorotrityl chloride resin (0.5 mmol g^{-1}). Diisopropylethylamine (DIEA)/HBTU were used to enhance coupling efficacy of the Fmoc-protected amino acid. Fmoc protecting group was deprotected by 20% piperdine/dimethyl formamide (DMF) (v/v). The peptide was cleaved from resin with a cleavage cocktail of trifluoroacetic acid (TFA), phenol, DI water, thioanisole, and ethanedithiol (EDT) in the volume ratio of 83:6.3:4.3:4.3:2.1 for 1.5 h. The filtrate was concentrated and precipitated in cold ether to obtain

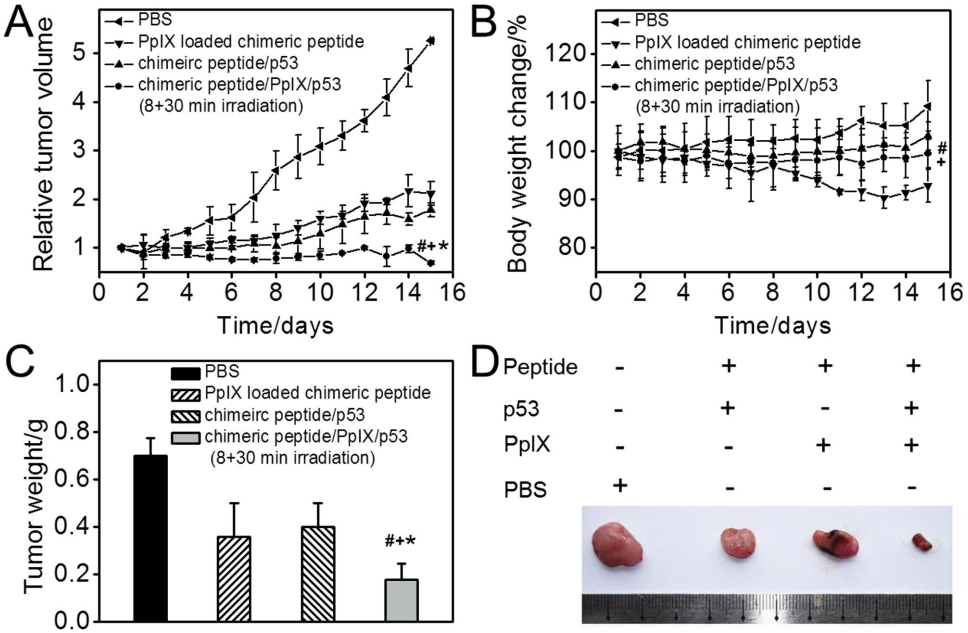

Figure 7. In vivo long-term antitumor study. A) Relative tumor volume in different groups after post-treatment; B) body weight changes when the mice were treated with different samples; C) the tumor weights at the 15th day post-treatment; D) Representative images of the tumors at the 15th day post-treatment. The mice groups of PBS, PpIX loaded chimeric peptide and chimeric peptide/p53 received 38-min light irradiation, while the group of chimeric peptide/PpIX/p53 received dual-stage light irradiation (8 + 30 min). $*p < 0.05$, $+p < 0.05$ and $\#p < 0.05$ when the group was compared with that treated with PpIX loaded chimeric peptide, PBS, and chimeric peptide/p53 DNA respectively as determined by a Student's *t*-test.

the white solid. The solid was dissolving precipitated repeatedly and then got dried under vacuum for 24 h. The final product was freeze-dried. The molecular weights were determined by ESI–MS (Finnigan LCQadvantage).

Cell Culture and Amplification of Plasmid DNA: SCC-7 and COS7 cells were incubated in Dulbecco's Modified Eagle Medium (DMEM) in an atmosphere of 5% CO_2 at 37 °C. The medium included 1% antibiotics (penicillin-streptomycin, 10 000 U mL^{-1}) and 10% heat-inactivated FBS.

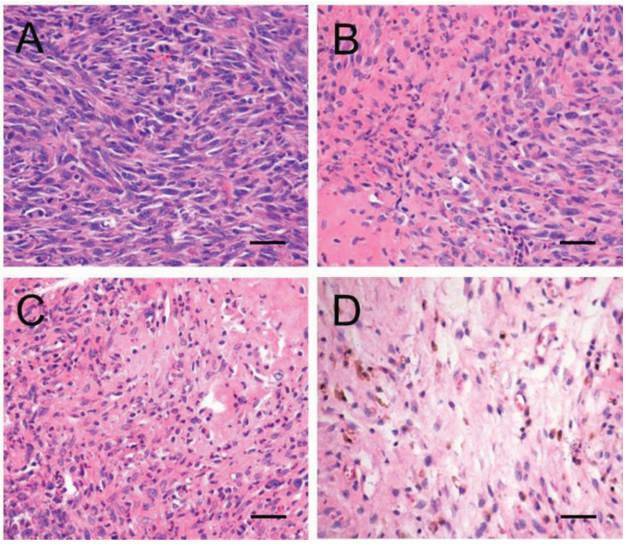

Figure 8. H&E staining of tumor tissues at the 15th day after treatment of various samples. A) PBS; B) PpIX loaded chimeric peptide; C) chimeric peptide/p53 complexes; D) chimeric peptide/PpIX/p53 complexes. The scale bar was 50 μm.

pGL-3 plasmid (reporter gene) and p53 expression plasmid (p53 DNA) were obtained as previous report.[23]

Drug Loading and Drug Release In Vitro: PpIX loaded chimeric peptide was prepared via a solvent evaporation method.[30] 1.8 mg of PpIX were dissolved in 1 mL of tetrahydrofuran (THF). And then the THF solution was added dropwise to distilled water with 0.5 mg mL^{-1} chimeric peptide (pH 7.4). The mixture was sonication for 20 min and stirred for 48 h at room temperature. The residual THF was removed by rotary evaporation. The mixture was centrifuged at 12000 rpm for 20 min. The solution was filtered with a 0.8 μm syringe filter and then used for in vitro and in vivo study. For in vitro release test at 37 °C at pH 7.4 and 5.0, respectively, the PpIX loaded solution was added to the dialysis tube (MW 1000 Da), and then directly immersed into 10 mL of buffer solution. At the predetermined time intervals, the buffer solution was replaced. The release amount of PpIX in buffer solution was determined on the basis of the UV–vis absorbance intensity at 407 nm. Besides, certain chimeric peptide solution before drug release test was lyophilized and dissolved in dimethylsulfoxide (DMSO), and the corresponding UV absorbance value was determined to calculate the mass of PpIX loaded in chimeric peptide. DLE and EE were defined as follow:

$$\text{DLE} = (\text{mass of drug loaded in chimeric peptide} / \text{mass of chimeric peptide}) \times 100\%$$

$$\text{EE} = (\text{mass of drug loaded in chimeric peptide} / \text{mass of drug fed initially}) \times 100\%$$

Chimeric Peptide/DNA Complexes Formation: 1 μg of DNA (200 ng μL^{-1} in Tris-HCl buffer solution) was directly mixed with appropriate volumes of peptide or PpIX loaded peptide. The solution was subsequently diluted to a total volume of 100 μL with PBS buffer solution (pH 7.4). The complexes were vortex vigorously for 5 s and incubated at 37 °C for 30 min. The complexes were used immediately after preparation.

Agarose Gel Electrophoresis Assay: Chimeric peptide/pGL-3 complexes at various w/w ratios were loaded onto the 0.7% (w/v) agarose gel containing GelRed. This assay was conducted with tris-acetate (TAE)

running buffer at 80 V for 60 min and measured through the Vilber Lourmat imaging system (France).

Particle Size and Zeta Potential Measurement: Nano-ZS ZEN3600 (Malvern Instruments) was employed to determine the particle size and zeta potential at 25 °C. Particle size and zeta potential were measured in PBS buffer (pH 7.4). The zeta potential of complexes in the presence of MMP-2 enzyme (0.12 μg mL^{-1}) at the w/w ratio 20 was measured. Data were given as mean ± standard deviation (SD) based on four independent measurements.

TEM Observation: Morphology of various samples (in PBS buffer, pH 7.4, 5 mM) with w/w ratio of 20 in the absence of MMP-2 enzyme and after coincubation with MMP-2 enzyme for 1 h was observed by TEM (JEM-2100 microscope). 0.2% (w/v) Phosphotungstic acid solution was used to stain the samples.

Gene Transfection In Vitro: Gene transfection of pGL-3 plasmids was studied against SCC-7 and COS7 cells. 25 kDa PEI was used as a positive control. Cells were seeded in the 24-well plate (6×10^4 cells/well). 24 h later, chimeric peptide/pGL-3 complexes at various w/w ratios were added to the each plate. The content of pGL-3 was 1 μg. After incubated for another 6 h, the medium was replaced with fresh medium containing 10% FBS. 48 h later, the medium was removed and cells were washed gently with PBS. Then the cells were cracked. The luciferase expression was measured by the luciferase assay system. The light manipulated gene transfection was conducted in the similar way. The only difference was the cells got 8 min light irradiated after chimeric peptide/PpIX/pGL-3 complexes were endocytosis for 6 h (band filter: 400–700 nm). The final concentration of PpIX was 0.44 mg L^{-1}.

Cytotoxicity Assay: The MTT assay was used to determine the cytotoxicity of various samples in SCC-7 cells. Generally, the cells were seeded at a density of 6000 cells/well and allowed to grow on a 96-well plate for 24 h in 100 μL DMEM containing 10% FBS. And then samples with various concentrations were added to each well. After incubated for 48 h, the medium was replaced with 200 μL fresh medium and 20 μL MTT (5 mg mL^{-1} in PBS buffer) solution. 4 h later, the medium was replaced with 200 μL DMSO. The absorbance at 570 nm was measured. The cell viability was defined as the percentage of survival cells per total nontreated cells. Specially, the dark toxicity of PpIX loaded chimeric peptide was determined without light irradiation, while the phototoxicity was determined in the condition that the cells got 60 min light irradiated after the samples were added for 6 h. Besides, the synergistic cytotoxicity of chimeric peptide/PpIX/p53 complexes was measured under dual-stage light irradiation, namely 8 min light irradiation after 6 h endocytosis and 52 min light irradiation after 40 h incubation.

CI Determination: CI was calculated as: $CI_x = D_1/Df_1 + D_2/Df_2$. Df_1 or Df_2 was the dose of drug 1 or drug 2 required to induce *x* percent effect alone, respectively. And D_1 or D_2 was the drug 1 or drug 2 required to induce the same *x* percent effect in the codelivery system.

Cellular Internalizaion Observation: CLSM was employed to investigate the cellular uptake behavior of chimeirc peptide/pGL-3 complexes in SCC-7 and COS7 cells. The cells were seeded in the 6-well plate at a density of 1×10^5 cells/well. After incubated for 24 h at 37 °C, the pGL-3 (1 μg) was labeled with YOYO-1 (5 μL, 1×10^{-6} M) for 15 min, and then 20 μL of 1 mg mL^{-1} chimeric peptides and 75 μL PBS (pH 7.4, 10×10^{-3} M) were added. The YOYO-1 labeled chimeric peptide/pGL-3 complexes were prepared by incubation for 30 min. The complexes were diluted to 1 mL in the absence or presence of MMP-2 inhibitor and added to the cells. After 6 h, the medium was removed and cells were washed with PBS three times. Thereafter, the cell nucleus was stained with 10 μL Hoechst 33342 (1 mg mL^{-1} in DMEM solution) for 15 min. Cells were washed with PBS three times again. And the fluorescence was analyzed by CLSM (C1-Si, Nikon, Japan).

Endosomal Escape Observation: Endosomal escape behaviors were observed in SCC-7 cells by CLSM. YOYO-1 labeled chimeric peptide/pGL-3 complexes or chimeric peptide/PpIX/pGL-3 complexes were added to the cells. After 6 h, the medium was replaced with DMEM and the cells were light irradiated for 0, 8, and 15 min, respectively. Subsequently, the endo/lysosomes were stained with LysoTracker Blue (6 μL, 50×10^{-9}M) for 40 min. The cells were washed with PBS for three times before observation.

Flow Cytometery: SCC-7 cells were seeded in the 6-well plate at a density of 1×10^5 cells/well and incubated at 37 °C for 24 h. And then 1 mL YOYO-1 labeled chimeric peptide/pGL-3 complexes were added in the absence or presence of MMP-2 inhibitor. After 6 h, the medium was removed. The cells were rinsed with PBS thoroughly. Subsequently, the cells were collected and resuspended in 500 μL PBS three times. The samples were determined on a Beckman Flow Cytometer (Epics XL). The results were analyzed with Flowjo 7.6 software. The codelivery of PpIX and DNA was studied in the similar manner. The bandpass filter used to detect PpIX fluorescence was 630 ± 11 nm.

In Vivo Antitumor Study: All animal experiments were performed according to the guidelines for laboratory animals established by the Wuhan University Center for Animal Center Experiment/A3-Lab. Mice were injected with SCC-7 cells. Once the tumors reached an approximate size of 100 mm^3, the mice were randomized divided into 4 groups, and each group was 6 mice. The mice were intratumorally injected with various samples (120 μL), including PBS buffer, chimeric peptide/p53 complexes, PpIX loaded chimeric peptide and chimeric peptide/PpIX/p53 complexes. The w/w ratio of chimeric peptide and p53 was 20. The EE value was 5.8%. The doses of p53 DNA and PpIX were 15 and 7 μg per mouse respectively. The mice that injected with chimeric peptide/PpIX/p53 complexes were treated by dual-stage light irradiation (8 min light irradiation after 6 h endocytosis and 30 min light irradiation after 24 h) using 630 nm He–Ne laser. While the mice injected with PpIX loaded chimeric peptide were also treated with 38 min light irradiation in total. The tumor size and mice weight were measured immediately before injection. The volume was defined as: $V = ((\text{tumor length}) \times (\text{tumor width})^2)/2$. Relative tumor volume was defined as V/V_0 (V_0 was the tumor volume when the treatment was initiated).[31,32] After the tumor tissues were sacrificed, H&E staining was used for further histological examinations. Statistical analysis was performed using a Student's *t*-test. The differences were considered significant for p value <0.05.

Supporting Information

Supporting Information is available from the Wiley Online Library or from the author.

Acknowledgements

This work was financially supported by the National Natural Science Foundation of China (51125014 and 51233003), National Key Basic Research Program of China (2011CB606202), the Ministry of Education of China (20120141130003), and Fundamental Research Funds for the Central Universities of China.

Received: September 14, 2014
Revised: November 19, 2014
Published online: January 13, 2015

[1] Y. Y. Yuan, J. Liu, B. Liu, *Angew. Chem. Int. Ed.* **2014**, *126*, 7291.
[2] T. Y. Jiang, R. Mo, A. Bellotti, J. P. Zhou, Z. Gu, *Adv. Funct. Mater.* **2014**, *24*, 2295.
[3] N. Wiradharma, Y. W. Tong, Y. Y. Yang, *Biomaterials* **2009**, *30*, 3100.
[4] H. Y. Wang, Q. Q. Guo, Y. F. Jiang, E. G. Liu, Y. X. Zhao, H. X. Wang, Y. P. Li, Y. Z. Huang, *Adv. Funct. Mater.* **2013**, *23*, 6068.
[5] A. C. Misra, S. Bhaskar, N. Clay, J. Lahann, *Adv. Mater.* **2012**, *24*, 3850.
[6] H. J. Yu, Y. L. Zou, Y. G. Wang, X. N. Huang, G. Huang, B. D. Sumer, D. A. Boothman, J. M. Gao, *ACS Nano* **2011**, *5*, 9246.
[7] Y. Y. Won, R. Sharma, S. F. Konieczny, *J. Controlled Release* **2009**, *139*, 88.
[8] L. M. Zhang, Z. X. Lu, Q. H. Zhao, J. Huang, H. Shen, Z. J. Zhang, *Small* **2011**, *7*, 460.

[9] M. J. Lee, A. S. Ye, A. K. Gardino, A. M. Heijink, P. K. Sorger, G. MacBeath, M. B. Yaffe, *Cell* **2012**, *149*, 780.
[10] J. F. Lovell, T. W. B. Liu, J. Chen, G. Zheng, *Chem. Rev.* **2010**, *110*, 2839.
[11] G. Pasparakis, T. Manouras, M. Vamvakaki, P. Argitis, *Nat. Commun.* **2014**, DOI: 10.1038/ncomms4623.
[12] M. K. G. Jayakumar, A. Bansal, K. Huang, R. S. Yao, B. N. Li, Y. Zhang, *ACS Nano* **2014**, *8*, 4848.
[13] T. Nomoto, S. Fukushima, M. Kumagai, K. Machitani, Y. Matsumoto, M. Oba, K. Miyata, K. Osada, N. Nishiyama, K. Kataoka, *Nat. Commun.* **2014**, *5*, 3545.
[14] H. B. Chen, L. Xiao, Y. Anraku, P. Mi, X. Y. Liu, H. Cabral, A. Inoue, T. Nomoto, A. Kishimura, N. Nishiyama, K. Kataoka, *J. Am. Chem. Soc.* **2014**, *136*, 157.
[15] K. Raemdonck, B. Naeye, K. Buyens, R. E. Vandenbroucke, A. Høgset, J. Demeester, S. C. D. Smedt, *Adv. Funct. Mater.* **2009**, *19*, 1406.
[16] A. K. Varkouhi, G. Mountrichas, R. M. Schiffelers, T. Lammers, G. Storm, S. Pispas, W. E. Hennink, *Eur. J. Pharm. Sci.* **2012**, *45*, 459.
[17] F. F. An, W. P. Cao, X. J. Liang, *Adv. Healthcare Mater.* **2014**, *3*, 1162.
[18] H. Parhiz, W. T. Shier, M. Ramezani, *Int. J. Pharm.* **2013**, *457*, 237.
[19] T. R. Pearce, K. Shroff, E. Kokkoli, *Adv. Mater.* **2012**, *24*, 3803.
[20] H. Y. Wen, C. Y. Dong, H. Q. Dong, A. J. Shen, W. J Xia, X. J. Cai, Y. Y. Song, X. Q. Li, Y. Y. Li, D. L. Shi, *Small* **2012**, *8*, 760.
[21] L. Zhu, P. Kate, V. P. Torchilin, *ACS Nano* **2012**, *6*, 3491.
[22] J. Zhang, Z. F. Yuan, Y. Wang, W. H. Chen, G. F. Luo, S. X. Cheng, R. X. Zhuo, X. Z. Zhang, *J. Am. Chem. Soc.* **2013**, *135*, 5068.
[23] K. Han, S. Chen, W. H. Chen, Q. Lei, Y. Liu, R. X. Zhuo, X. Z. Zhang, *Biomaterials* **2013**, *34*, 4680.
[24] D. W. Pack, A. S. Hoffman, S. Pun, P. S. Stayton, *Nat. Rev.* **2005**, *4*, 581.
[25] S. Y. Berezhna, L. Supekova, F. Supek, P. G. Schultz, A. A. Deniz, *Proc. Natl. Acad. Sci. U.S.A.* **2006**, *103*, 7682.
[26] S. Yang, S. May, *J. Chem. Phys.* **2008**, *129*, 185105.
[27] A. M. Sauer, A. Schlossbauer, N. Ruthardt, V. Cauda, T. Bein, C. Bräuchle, *Nano Lett.* **2010**, *10*, 3684.
[28] X. C. Ma, X. B. Wang, M. Zhou, H. Fei, *Adv. Healthcare Mater.* **2013**, *2*, 1638.
[29] K. Han, Y. Liu, W. N. Yin, S. B. Wang, Q. Xu, R. X. Zhuo, X. Z. Zhang, *Adv. Healthcare Mater.* **2014**, *3*, 1765.
[30] X. Shuai, H. Ai, N. Nasongkla, S. Kim, J. Gao, *J. Controlled Release* **2004**, *98*, 415.
[31] Z. Liu, A. C. Fan, K. Rakhra, S. Sherlock, A. Goodwin, X. Y. Chen, Q. W. Yang, D. W. Felsher, H. J. Dai, *Angew. Chem. Int. Ed.* **2009**, *48*, 7668.
[32] J.-H. Park, G. von Maltzahn, L. L. Ong, A. Centrone, T. A. Hatton, E. Ruoslahti, S. N. Bhatia, M. J. Sailor, *Adv. Mater.* **2010**, *22*, 880.